Economic Comparison of Continuous and Batch Sintering of Silicon Nitride

Continuous sintering has recently been investigated as a means for cost-effective sintering of selected Si_3N_4 compositions. Factors related to the cost of sintering in both belt furnaces and batch furnaces of increasing capacity—to allow sintering of the large number of parts required by the automotive industry—have been considered.

DALE E. WITTMER,* JOSEPH J. CONOVER, AND VINCENT A. KNAPP
Southern Illinois University, Carbondale, Illinois 62901

CHARLES W. MILLER, JR.*
Centorr Furnaces/Vacuum Industries, Nashua, New Hampshire 03063-1016

It is generally agreed that Si_3N_4-based compositions can be produced with reliable properties that are suitable for some automotive components. The major barrier to extensive application of Si_3N_4 components is cost. In a recent economic study concerning the cost of producing Si_3N_4 cam-roller followers and turbocharger rotors,[1] the major costs were broken down into the following components: materials, energy, labor, capital, and other. In their study, Das and Curlee[1] focused on the effect of low-cost powders on the economic viability of Si_3N_4-based compositions replacing metal components in automotive applications. A conclusion reached from their economic modeling was that technological advances are required in all areas of production for ceramic components to be competitive with metals.

The major areas which are expected to achieve technological advancement to make low-cost components for the automotive industry a reality are raw material (primarily the cost of the Si_3N_4 powder), powder processing, sintering, machining, and nondestructive evaluation.

Previously, Wittmer and Miller[2] and Wittmer, Paulson, and Miller[3] showed that it is feasible to sinter large Si_3N_4 disks (100–150 g) to full density in a continuous furnace in flowing N_2. A comparison was made between continuous sintering in a commercial belt furnace and sintering in a conventional batch furnace, for the same time and temperature. The composition investigated was A4Y13–Si_3N_4 (Si_3N_4 containing 4 wt% Al_2O_3 and 13 wt% Y_2O_3 sintering aids) with sintering occurring at about 1670°C for 90 min in flowing N_2.

For the Si_3N_4 sintered in the belt furnace, the average four-point flexural strength was found to be 969 ± 45 MPa with a Weibull modulus of 21, and the fracture toughness by modified indentation was 7.2 ± 0.5 MPa·$m^{1/2}$. For the batch furnace, the average four-point flexural strength was found to be only 718 ± 132 MPa with a Weibull modulus of 5.5, and the fracture toughness by modified indentation was 5.9 ± 1.0 MPa·$m^{1/2}$. Since this work, additional formulations of Si_3N_4, containing reduced amounts of sintering aids, have been successfully sintered in the belt furnace over the temperature range of 1625° to 1750°C for 30 to 90 min in flowing N_2.

Economic Comparison of Continuous and Batch Sintering

This section focuses on the sintering costs for two sizes of Si_3N_4 cam-roller followers. The small roller follower is the same as referred to by Das and Curlee,[1] whereas the large roller follower is the same as the narrow follower referred to by Kalish.[4] The dimensions of the

*Member, American Ceramic Society.

Table I. Furnace Hot-Zone Dimensions and Furnace Capacities for Belt and Batch Furnaces

Furnace type	Furnace hot-zone dimensions (cm)			Furnace capacity				Minimum floor space (m^2)
				Small roller		Large roller		
	Width	Height	Depth	No. of rollers	Total load (kg)	No. of rollers	Total load (kg)	
840BF	20.3	10.2	103.2	1280	55	320	52	15
880BF	20.3	10.2	206.4	2560	110	640	104	19
242436	61	61	91.4	12288	516	3456	620	17
242448	61	61	132.0	18432	773	4608	755	23

green form large roller follower are 47.9-mm OD, 1.9-mm ID, and 17.5-mm width; its weight is 44 g. The dimensions of the green form small roller follower are 23.3-mm OD, 0.9-mm ID, and 17.1-mm width; its weight is 12 g. These dimensions take into consideration 18% shrinkage during sintering and removal of 0.625 mm from all sintered surfaces during finishing.

A simple spreadsheet program was used to calculate only the costs relating to the sintering of a Si_3N_4 formulation that would densify for the conditions modeled. The major components used for calculating sintering cost were labor, capital (using 10-year straight-line depreciation), energy, inert gas, water, and other (furnace fixtures and replacement parts, not including the labor to replace them). To make direct comparisons of the costs related only to sintering, the following assumptions were made:

- The plant runs 3 shifts for 365 d/year.
- Labor includes only the time to run the minimum number of furnaces required to meet capacity, and does not include time to load and unload parts from the boats or the effects of downtime for maintenance and repair.
- Labor efficiency is based on the ability of one furnace operator to manage a maximum of four furnaces at one time, but a minimum of 50% of an operator's time is required to operate one furnace.
- Maximum furnace loading is based on using BN boats or trays with lids and no packing powders.

Table II. Costs for Small Cam-Roller Followers Sintered in Graphite Furnaces as Functions of Furnace Production and Yield

Furnace type	Part yield (%)	5 million rollers		10 million rollers		15 million rollers	
		No. of furnaces	$/roller	No. of furnaces	$/roller	No. of furnaces	$/roller
840	90	1	0.0314	1	0.0240	2	0.0263
	80	1	0.0334	2	0.0332	2	0.0283
	70	1	0.0360	2	0.0358	2	0.0309
880	90	1	0.0286	1	0.0192	1	0.0161
	80	1	0.0296	1	0.0204	1	0.0173
	70	1	0.0313	1	0.0219	1	0.0188
242436	90	2	0.0800	3	0.0611	4	0.0537
	80	2	0.0839	3	0.0643	4	0.0563
	70	2	0.0894	3	0.0682	4	0.0597
242448	90	1	0.0575	2	0.0573	3	0.0519
	80	1	0.0608	2	0.0606	3	0.0544
	70	1	0.0648	2	0.0646	3	0.0576

For comparison, models 840BF and 880BF belt furnaces and models 242436 and 242448 batch furnaces were selected. Model 840BF has a hot zone 20.3 cm wide × 10.2 cm high × 103.2 cm long, and model 880BF has the same cross section but is 206.4 cm long. Model 242436 is 61 cm wide × 61 cm high × 91.4 cm deep, and model 242448 has the same cross section but is 132 cm deep. The hot-zone dimensions for each furnace, with the loading capacities for both sizes of the cam-roller followers, are given in Table I.

For each furnace, the costs related to using either graphite or tungsten heating elements were considered. Sintering costs were calculated based on the yield of within-specification parts being 90%, 80%, or 70% of the total furnace production. For the belt furnaces, a constant sintering cycle of 60 min at 1750°C was selected, whereas for the batch furnaces, the cycle time was dependent on the furnace size and type of heating element. For instance, model 242436 with graphite heating elements took about 2 h longer to cool down than the same model with tungsten heating elements, due to the additional carbon felt insulation required. For all batch furnaces, the cycle consisted of evacuation and purge (0.5 or 0.75 h), ramp up (8 h), soak (4 h at 1750°C) and cool down (6 or 8 h).

The sintering costs determined for production yields of 90%, 80%, and 70% for 5 million, 10 million, or 15 million small cam-roller followers per year in each of the furnaces are given in Tables II and III, while those for sintering the same quantities of the larger cam-roller followers in the same furnaces are given in Tables IV and V.

Belt Sintering More Cost Effective

The data generated (for the two roller followers considered) from this economic model indicate that sintering in belt furnaces is more cost effective than sintering in batch furnaces, regardless of the furnace yield or type of hot zone. Figure 1(A) shows sintering as a function of yield for producing 15 million small

Table III. Costs for Small Cam-Roller Followers Sintered in Tungsten Furnaces as Functions of Furnace Production and Yield

Furnace type	Part yield (%)	5 million rollers		10 million rollers		15 million rollers	
		No. of furnaces	$/roller	No. of furnaces	$/roller	No. of furnaces	$/roller
840	90	1	0.0340	1	0.0252	2	0.0279
	80	1	0.0360	2	0.0358	2	0.0301
	70	1	0.0387	2	0.0385	2	0.0327
880	90	1	0.0324	1	0.0212	1	0.0175
	80	1	0.0337	1	0.0225	1	0.0187
	70	1	0.0352	1	0.0240	1	0.0203
242436	90	2	0.0949	3	0.0728	4	0.0641
	80	2	0.0988	3	0.0761	4	0.0669
	70	2	0.1046	3	0.0801	4	0.0704
242448	90	1	0.0652	2	0.0649	3	0.0594
	80	1	0.0685	2	0.0682	3	0.0620
	70	1	0.0727	2	0.0724	3	0.0653

cam-roller followers per year in different-sized graphite belt and batch furnaces. Figure 1(A) shows that the sintering cost for the 840 belt furnace is about 50% of that for the 242436 batch furnace, whereas for the 880 belt furnace sintering cost is about 30% of that for the 242448 batch furnace. Also, a reduction in yield produces a more pronounced effect of increased cost for sintering in the batch furnaces, compared to sintering in the belt furnaces.

For the same production in furnaces with tungsten heating elements, the behavior is quite similar, as shown in Fig. 1(B).

A comparison of the results illustrated in Figs. 1(A) and (B) shows that sintering in furnaces with graphite heating elements appears to be slightly more cost effective than sintering in furnaces with tungsten heating elements. However, there is some question on the effect of the furnace environment on the sintering behavior of some Si_3N_4 compositions. Recently, there has been evidence to suggest that the use of graphite heating elements and furnace insulation may require the use of setter powders which would increase sintering costs and might affect surface finish and overall yield.

The sintering costs for the production of 15 million large cam-roller followers (Figs. 1(C) and (D)) appear similar to those for the small cam-roller followers. However, the effect of reduction in furnace yield appears more pronounced, especially for the batch furnaces. For the 242436 batch furnace, there is about a 30% increase in cost for a furnace yield of 70% compared to 90%. The main reason for this increase is the need for a larger number of furnaces and the associated labor and replacement parts with

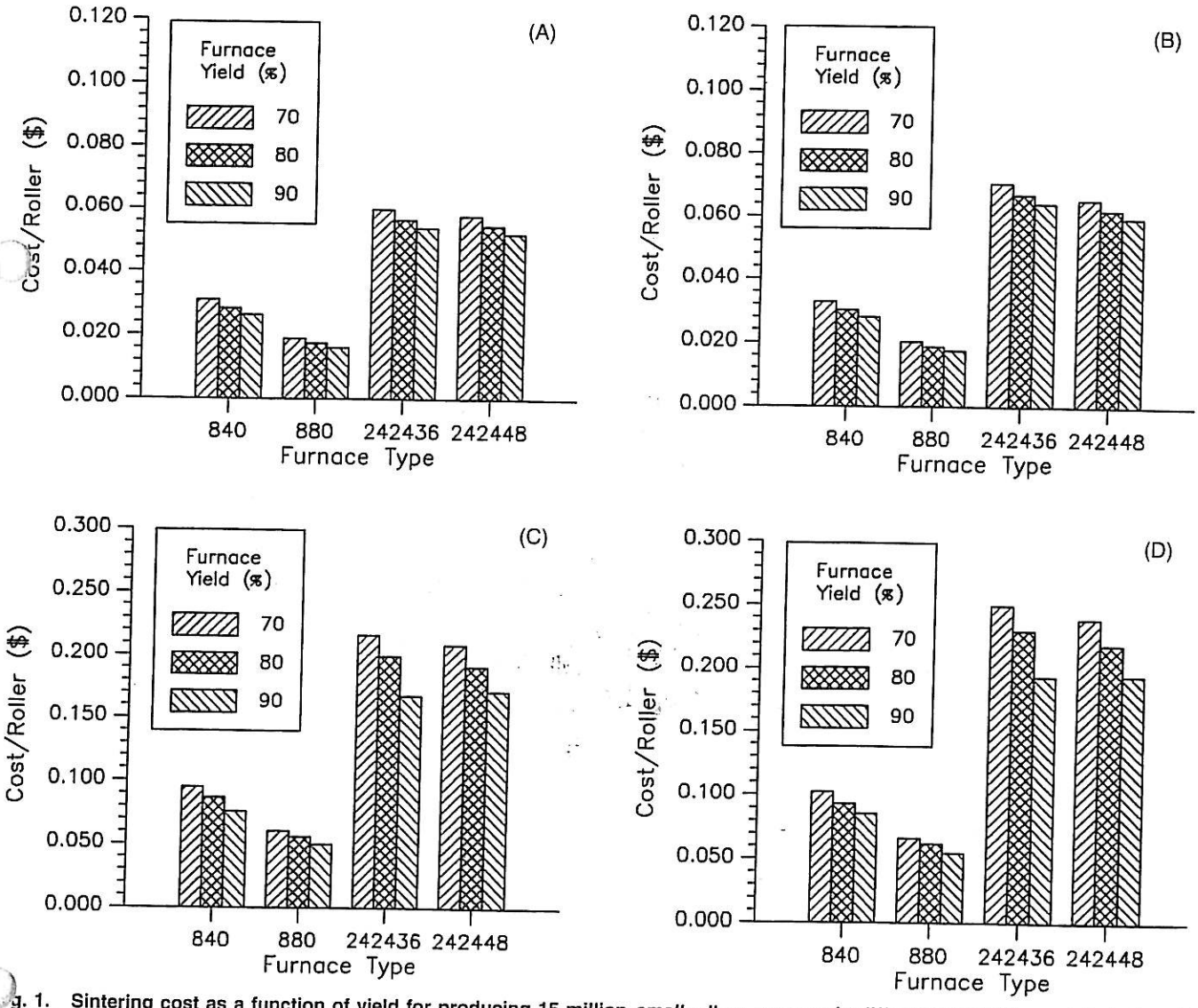

Fig. 1. Sintering cost as a function of yield for producing 15 million *small* rollers per year in different-sized (A) graphite belt and batch furnaces and (B) tungsten belt and batch furnaces. Sintering cost as a function of yield for producing 15 million *large* rollers per year in different-sized (C) graphite belt and batch furnaces and (D) tungsten belt and batch furnaces.

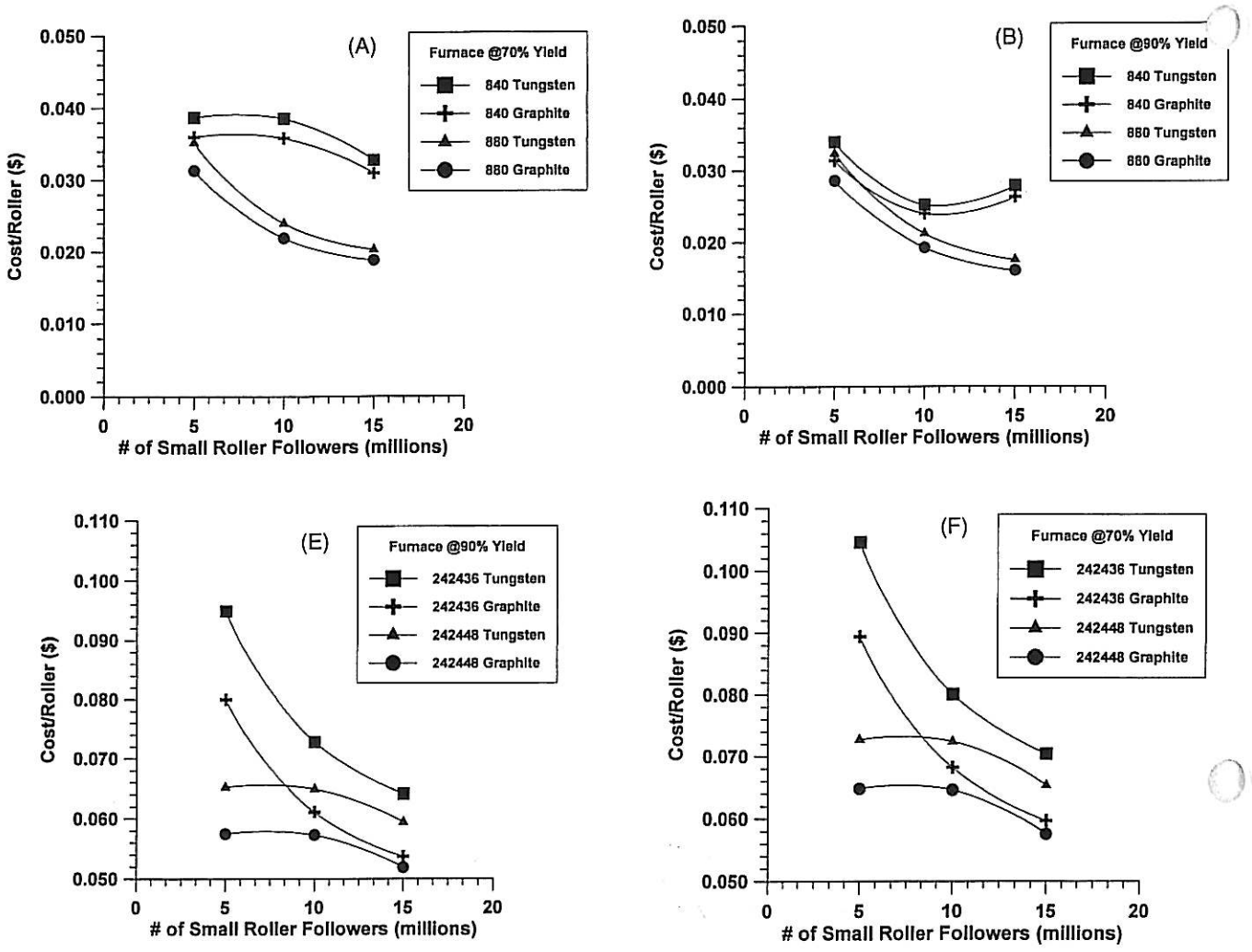

Fig. 2. Cost per roller as a function of production volume of *small* rollers sintered in graphite and tungsten belt furnaces operating at (A) 90% yield and (B) 70% yield. Cost per roller as a function of production volume of *large* rollers sintered in graphite and tungsten belt furnaces operating at (C) 90% yield and (D) 70% yield. Cost per roller as a function of production volume of *small* rollers sintered in graphite and tungsten batch furnaces operating at (E) 90% yield and (F) 70% yield. Cost per roller as a function of production volume of *large* rollers sintered in graphite and tungsten batch furnaces operating at (G) 90% yield and (H) 70% yield.

Table IV. Costs for Large Cam-Roller Followers Sintered in Graphite Furnaces as Functions of Furnace Production and Yield

		5 million rollers		10 million rollers		15 million rollers	
Furnace type	Part yield (%)	No. of furnaces	$/roller	No. of furnaces	$/roller	No. of furnaces	$/roller
840	90	2	0.0948	4	0.0760	6	0.0757
	80	3	0.1012	5	0.0936	7	0.0866
	70	3	0.1095	6	0.1091	8	0.0949
880	90	1	0.0574	2	0.0572	3	0.0499
	80	2	0.0810	3	0.0634	4	0.0558
	70	2	0.0870	3	0.0681	4	0.0602
242436	90	4	0.1728	8	0.1721	11	0.1673
	80	5	0.2316	9	0.2081	13	0.1991
	70	5	0.2477	10	0.2268	14	0.2161
242448	90	3	0.1717	6	0.1712	9	0.1712
	80	4	0.1991	7	0.1887	11	0.1912
	70	4	0.2100	8	0.2094	12	0.2087

Table V. Costs for Large Cam-Roller Followers Sintered in Tungsten Furnaces as Functions of Furnace Production and Yield

		5 million rollers		10 million rollers		15 million rollers	
Furnace type	Part yield (%)	No. of furnaces	$/roller	No. of furnaces	$/roller	No. of furnaces	$/roller
840	90	2	0.0100	4	0.0782	6	0.0851
	80	3	0.1094	5	0.1069	7	0.0928
	70	3	0.1175	6	0.1171	8	0.1020
880	90	1	0.0617	2	0.0615	3	0.0542
	80	2	0.0887	3	0.0694	4	0.0616
	70	2	0.0950	3	0.0746	4	0.0661
242436	90	4	0.2016	8	0.2006	11	0.1935
	80	5	0.2665	9	0.2400	13	0.2297
	70	5	0.2831	10	0.2618	14	0.2495
242448	90	3	0.1949	6	0.1941	9	0.194
	80	4	0.2294	7	0.2156	11	0.218
	70	4	0.2411	8	0.2400	12	0.2390

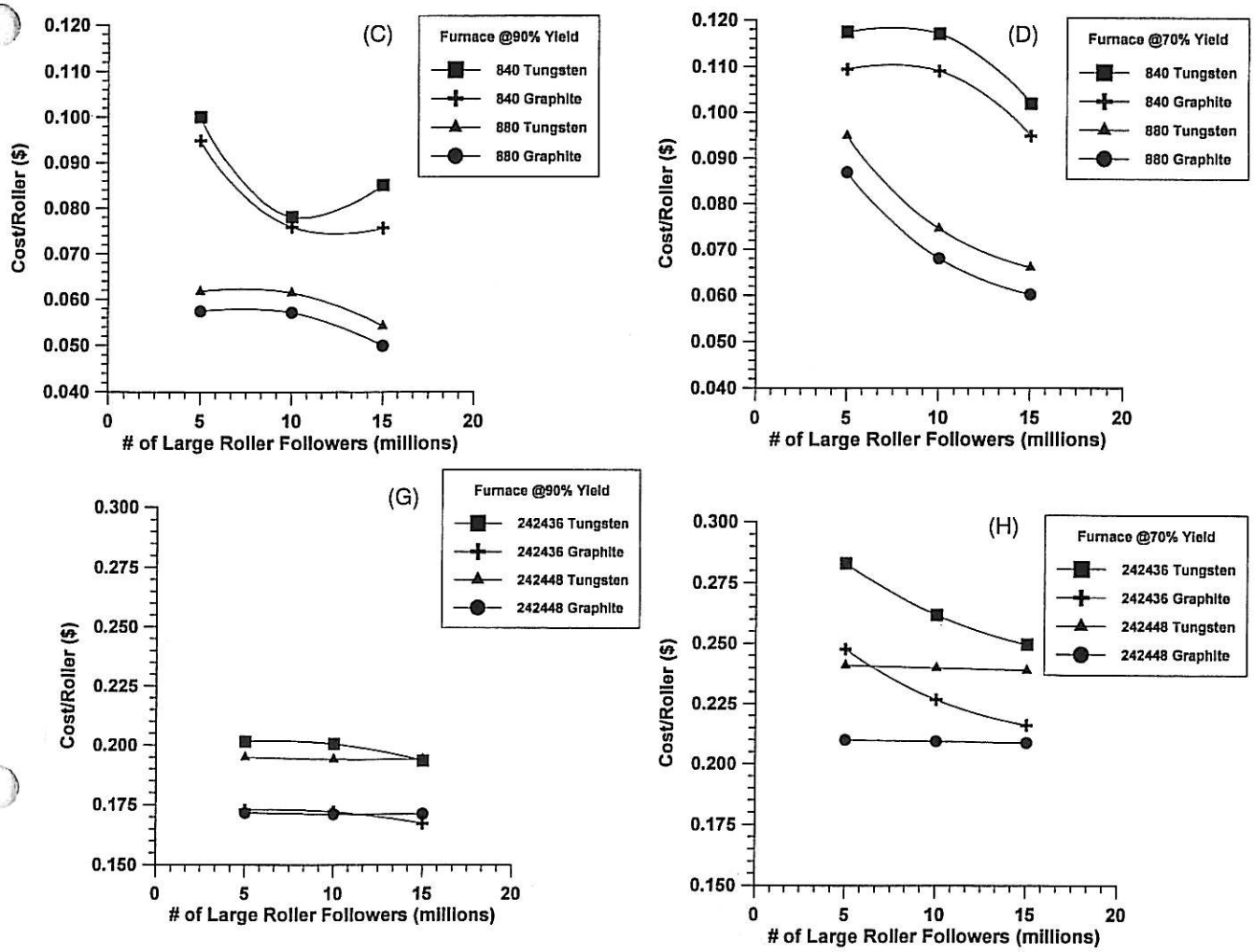

reduced yield.

Figures 2(A) to (F) illustrate the cost per roller as a function of production volume at fixed yield. Figure 2(A) shows that, for the four belt furnaces, at 90% yield, at low production levels, the sintering cost per small roller is about the same (near $0.03/roller), but, as the production quantity increases, the larger belt furnaces become more cost effective. At furnace yields of 90%, there is little difference in the cost per roller—at a production level of 15 million small rollers per year—between the larger graphite and tungsten belt furnaces; however, the smaller belt furnaces show increased cost with production quantity. This is due to the need for additional furnaces, operating at much less that peak capacity (for production >10 million rollers per year), which increases the capital costs. The same furnaces at 70% yield (Fig. 2(B)) show somewhat the same trends as at 90%, although, as expected, the cost per roller is somewhat higher.

These differences are magnified for sintering the large cam-roller followers. Figures 2(C) and (D) show that the sintering costs are much lower in the larger belt furnaces, compared to the smaller belt furnaces. Also, a reduction in furnace yield from 90% to 70% has a significant effect on sintering cost. In all cases, it appears that the larger graphite belt furnace is the most cost effective.

The results of comparing batch furnaces are not so straight forward. At low production levels at 90% yield for the small rollers (Fig. 2(E)), there is a wide variation in cost per roller, with the sintering cost in the smaller tungsten furnace (242436) being nearly double that of the larger graphite furnace (242448). As the production level increases, the cost per roller in the smaller graphite furnace approaches the cost per roller in the larger graphite furnace. This is due to the more efficient use of labor for a higher number of the smaller furnaces and the higher fixture and repair parts costs for the larger furnaces. As expected, reducing the furnace yield to 70% (Fig. 2(F)) increases the cost per roller, but has little effect on the basic trends observed for 90% yield.

For the large cam-roller follower, the cost per roller, as a function of production volume, for sintering in

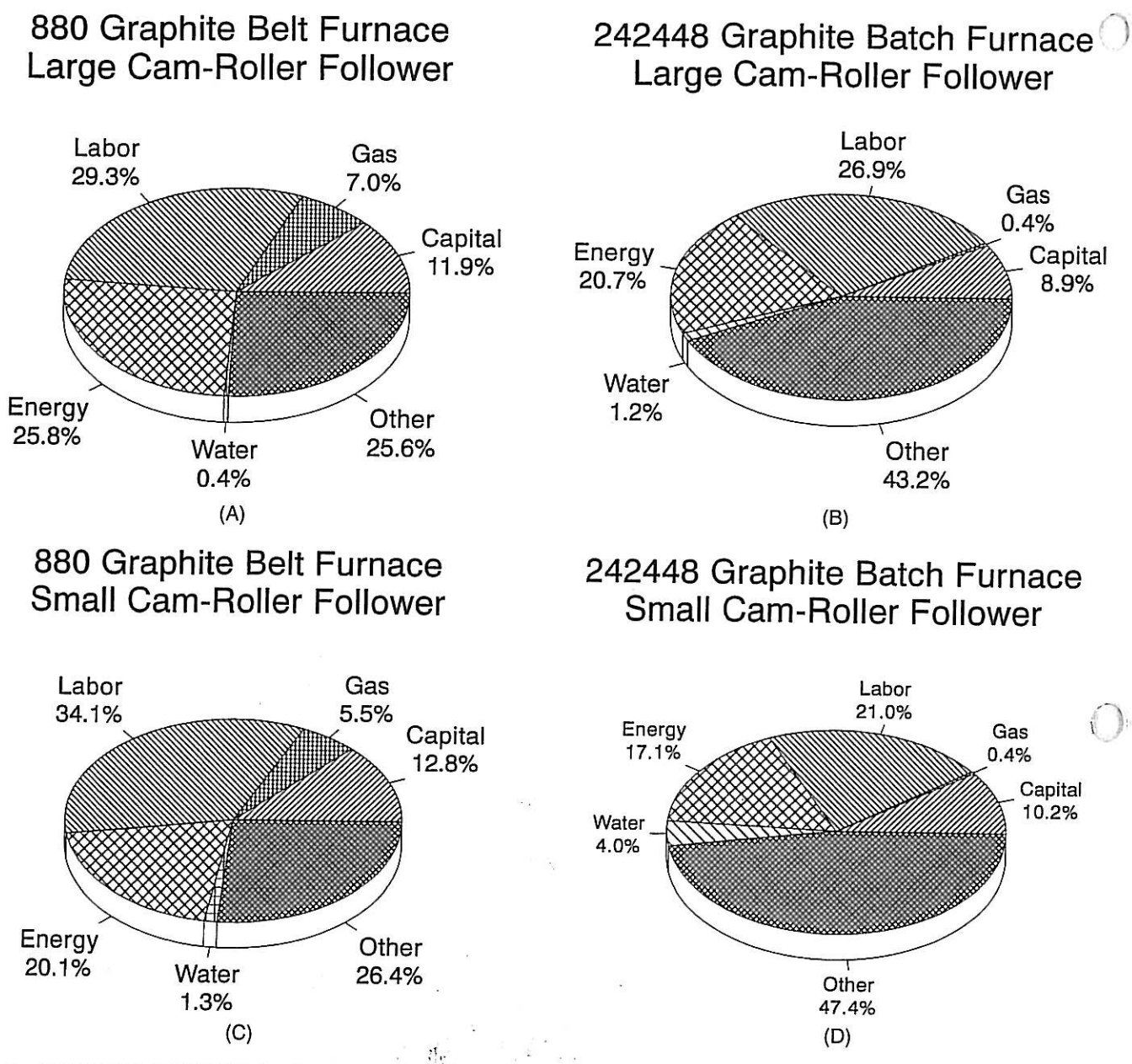

Fig. 3. Cost distribution for sintering *large* cam-roller followers in large graphite (A) belt and (B) batch furnaces. Cost distribution for sintering *small* cam-roller followers in large graphite (C) belt and (D) batch furnaces.

the batch furnaces, has a relatively flat behavior at 90% furnace yield (Fig. 2(G)). The cost per roller for the graphite batch furnaces is about the same with little cost variation with increased production volume, whereas the cost per roller is about 30% greater in the tungsten batch furnaces with little effect by furnace size. Reducing the furnace yield to 70% (Fig. 2(H)) creates a greater separation in cost at the low production level and shows more of a trend for reduced cost, as a function of increased production for the smaller batch furnaces, compared with the larger batch furnaces. As with the small rollers, at high production levels, the smaller graphite furnace is nearly as cost effective as the larger graphite batch furnace, due to more efficient use of labor and lower fixture and repair parts costs.

As mentioned previously, the major components used for determining cost are labor, capital, energy, gas, water, and other (furnace fixtures and replacement parts). Figures 3(A) and (B) represent typical cost breakdowns for sintering 15 million large cam-roller followers (90% yield) in graphite belt and batch

rnaces, respectively. Figure 3(A) shows that, for the 880 graphite belt furnace, labor (29.3%), energy (25.8%), and other (25.6%) costs are nearly equivalent, followed by capital (11.9%), gas (7.0%), and water (0.4%) costs. In comparison (Fig. 3(B)), for the 242448 graphite batch furnace, other cost is by far the most controlling category (43.2%), followed by labor (26.9%), energy (20.7%), capital (8.9%), water (1.2%), and gas (0.4%) costs. Similar cost breakdowns are observed for the small cam-roller followers, as shown in Figs. 3(C) and (D).

There are several reasons that sintering in belt furnaces is more cost effective than sintering in batch furnaces. The cycle time and thermal load remain constant through the belt furnace, whereas the cycle time for batch furnaces increases with increasing thermal load. To reduce thermal lag in a batch furnace, the heating rate must be reduced to minimize thermal gradients across the load cross section. Larger thermal loads also take longer to cool in batch furnaces, whereas the cooling rate for belt furnaces depends on transport speed through the furnaces.

For this economic model, fan-assisted cooling was used on the batch furnaces to minimize the cooling step. Table I shows that the number of parts in the furnace hot zone is almost a factor of 10 greater for the batch furnaces, compared to the belt furnaces; therefore, the fixturing costs are much greater for the batch furnaces. These quantities also indicate how many parts would be lost in a bad sintering run or during a furnace upset.

So far, comparisons have been made between sintering in belt furnaces and sintering in batch furnaces at the same furnace yields. It is well-known and accepted that the larger the batch furnace, the lower the expected furnace yield. The reduced yield is primarily due to the large thermal lag that exists between the parts and the furnace elements and the large temperature gradient that exists in the load during heating and cooling. To minimize temperature gradients, the heating and cooling rates need to be controlled, which adds to the sintering cycle time, and may have significant effects on the microstructure, surface reaction layers, and properties of the Si_3N_4 parts.

In determining furnace needs for specific production targets, there is also the question of furnace downtime on the effective furnace yield. Furnace downtime is for routine maintenance, bad furnace runs, and unexpected furnace interrupts (loss of power or gas and controller, thermocouple, or element failure, etc.). The amount of product loss includes the direct loss (parts in the furnace when it failed) plus the indirect loss (production lost due to the downtime). The direct loss is much more costly than the indirect loss, since it includes the material and processing costs that have been invested in the part, up to and including the sintering.

In the belt furnaces, changes in operating conditions and onset of furnace failure are more easily detected and corrected than in batch furnaces. From experience with furnace failures, there is less product lost and less downtime to affect total production in the case of furnace upsets in belt furnaces compared with batch furnaces. When a problem is detected in a belt furnace, the furnace can be purged of the parts in the run, cooled, repaired, and brought back to operation in less than 4–8 h. Direct and indirect product losses can be kept to a minimum for the belt furnace.

For example, using the information in Tables I and IV and assuming an 8-h upset, an 880 graphite belt furnace (operating at 90% yield), sintering the large cam-roller followers, sustains a direct loss of the 320 rollers in the furnace plus an indirect loss of 4562 rollers, for a total loss of 4882 rollers for the event. Assuming $2.0499/roller (including powder and processing costs), the direct loss is $656, and the indirect loss (production loss × sintering cost/roller × percent of capital cost) is about $27 for a total of about $683 for the upset.

For batch furnaces the downtime is much longer (usually 24 h or longer) due to the greater thermal load that requires longer cooling times (8 h), having to unload and reload parts (2 h), time to make repairs (4 h), and the time required to bring the furnace back up to operating conditions (10 h). Also, there are additional parts which require maintenance, such as vacuum pumps and seals, and loading devices.

For example, in a typical 24-h upset, a 242448 graphite batch furnace (operating at 90% yield) sintering the large cam-roller followers sustains a direct loss of 4608 rollers in the furnace plus an indirect loss of 4732 rollers, for a total loss of 9341 rollers lost for the event.

Assuming $2.1712/roller (including powder and processing cost), the direct loss is $10,005, and the indirect loss is $728, for a total of $10,733 for the event.

From experience with sintering of Si_3N_4 compositions in both belt and batch furnaces, it is more realistic to compare yields of 90% from the belt furnaces with 80%, 70%, or 60% yields from the batch furnaces, depending on the furnace size and sintering conditions. However, the above examples have made the point that, for equivalent production yields, belt furnaces are much more cost effective with respect to both sintering cost and costs related to upsets or downtime. To make this scenario reality requires that the Si_3N_4 composition be sinterable in the belt furnace and possess physical properties adequate for the intended application.

Results from Continuous Sintering of Si_3N_4

The goal of recent work involving continuous sintering has been to determine the feasibility of sintering Si_3N_4 compositions containing reduced amounts

of sintering aids. Since the high-temperature properties of Si_3N_4 are related to the amount and degree of crystallization of the liquid-phase formers during sintering, reducing the amounts of sintering aids should improve the high-temperature performance. The results presented here are meant only to summarize some of the compositions and properties for formulations that have been successfully sintered in the belt furnace. A more detailed discussion of this work will be presented in future publications.

Procedure

Commercially available Si_3N_4 powders (LC10 and LC12 grades, Hermann C. Starck, Berlin, Germany; E10 grade, UBE Industries America, New York, and ASN34 grade, Performance Ceramics, Peninsula, OH), containing 2–4 wt% Al_2O_3 (HPA-0.5 AF grade, Ceralox Corp., Tuscon, AZ) in combination with 6–13 wt% Y_2O_3 (high-purity grade, Hermann C. Starck) or 6–8 wt% La_2O_3 (high-purity grade, Molycorp, Inc., White Plains, NY) were processed by turbomilling* and pressure casting. This procedure has been discussed in detail in previous work.[5–8] After they were dried and isopressed, the disks (approximately 9 cm in diameter × 2 cm thick and weighing 100–125 g) were sintered in a commercial belt furnace (Model 6-BF, Centorr Furnaces/Vacuum Industries, Nashua, NH) over the temperature range 1625°–1750°C for 30–90 min in flowing N_2. These disks were sintered between BN plates inside of molybdenum boats, without the use of setter or packing powders. The heating rate, controlled by the belt speed and temperature of the hot zone, was generally in the range 100°–150°C/min from 250°C up to the peak temperature.

After sintering, the density of the disks was determined by the Archimedes method. The best sintered densities obtained for several of the compositions tested are given in Table VI. Disks with high densit were machined into standard 3 mm × 4 mm × 45 mm test bars for four-point flexural strength and fracture toughness measurements.

Table VI. Sintered Densities of Si_3N_4 Compositions Sintered in the Belt Furnace

Composition*	Firing temperature (°C)	Firing time (min)	Percent of theoretical density
A4Y6–LC10	1700	60	95.6
A4Y6–LC12	1725	90	98.5
A4Y6–E10	1700–1750	60–90	99.5
A2Y8–LC10	1750	90	89.5
A2Y8–E10	1750	90	100
A4L6–LC10	1675	60	93.4
A4L6–LC12	1700	60	96.4
A4L6–E10	1750	90	99.1
A2L8–LC10	1750	90	92.9
A2L8–E10	1725–1750	90	99.1
A4Y13–LC10	1600–1650	90	98.1–99.5
A4Y13–E10	1625–1725	60–90	99.4–100
A4Y13–ASN-34	1675–1725	30–90	99.7–100
A4Y13–E10 5% β-Si_3N_4 seed	1625–1725	30–90	99.4–99.6

*A is Al_2O_3, Y is Y_2O_3, L is La_2O_3; numeral following A, Y, and L is composition in wt%. LC10, LC12, E10, and ASN34 are commercial Si_3N_4.

Discussion

The results given in Table VI indicate that several of these compositions achieved densities >98% of theoretical, under sintering conditions (times and temperatures) significantly less stringent than typically required for such compositions. For compositions containing 10% or less sintering aids, general sintering practice dictates the use of packing powders, N_2 overpressure, temperatures in excess of 1800°C, and times greater than 2 h.

Crosbie *et al.*[9] compared intermediate hold temperatures, heating rates of 100°C/h (1.67°C/min) and 600°C/h (10°C/min), and hold time at peak temperature (1 and 2 h) on the sintering behavior of Si_3N_4 (E10), containing 2.26 wt% Al_2O_3 and 10 wt% Y_2O_3 sintering aids. The Si_3N_4 was embedded in a packing powder and sintered in a conventional tungsten-heated cold-wall batch furnace. The atmosphere was vacuum to 1100°C and then slight N_2 overpressure for the rest of the run at the peak sintering temperature of 1800°C. Crosbie *et al.* concluded that the higher heating rate had the most significant effect on density and associated properties, although longer times and higher intermediate hold temperature also were positive factors.

The heating rate developed during continuous sintering in the belt furnace is at least an order of magnitude greater than that of the maximum rate used by Crosbie *et al.*[9] and more than double the rate possible in small laboratory-sized batch furnaces. It is believed that the rate of liquid formation, due to the high heating rate possible in the belt furnace, enhances both the rearrangement and solution–precipitation mechanisms of liquid-phase sintering. This enhanced liquid-phase sintering is thought responsible for producing near theoretical density at reduced times and temperatures. Also, the use of setter powders is not required because densification proceeds rapidly to the point of closed porosity, thereby essentially reducing the overall surface area available for decomposition. In support of this theory, weight loss for nearly all compositions sintered in the belt furnace have been <0.5 wt%, and the microstructures contain uniformly distributed, well-rounded, fine porosity (even for sintering times of only 30 min).

Properties

Typical room-temperature physical property results for some of the compositions investigated are given in Table VII. The techniques for measuring these properties is given elsewhere.[6] Where a single value is

*The turbomill is a high-shear milling apparatus from Noble Technologies Group, Gilmanton, NH.

Table VII. Sintering Conditions and Physical Property Results for Compositions Sintered in the Belt Furnace

Composition*	Sintering conditions: Temperature (°C)	Sintering conditions: Time (min)	Percent of theoretical density	Modulus of rupture (MPa)	K_{IC} (MPa·m$^{1/2}$): Ref. 10	K_{IC} (MPa·m$^{1/2}$): Ref. 11
A4Y6–E10	1700	60	99.9	870–926	5.5	6.5
A4Y6–LC10	1700	60	96	917–1021	7.9	6.7
A4Y6–LC12	1725	90	98.8	778–938	5.7	6.2
A2Y8–E10	1750	90	100	926–1036	10.3	7.3
	1700	90	99.0	1004–1118	9.6	7.1
		30	94.4	850–1051	7.1	6.2
	1625	90	93.7	880	7.4	6.5
A2L8–E-10	1750	90	98.5	683–866	7.9	6.7
	1725	90	99.0	896–995	8.0	6.8
A4Y6L7–E10	1725	90	98.1	755–965	6.5	6.0
	1700	90	99.0	962–982	8.3	6.9
	1625	90	98.3	907–1041	8.0	6.6
A4Y13–LC10	1625	90	99.5	969	7.2	6.5
A4Y13–E10	1725	90	99.8	784–1121	12.9	6.5
	1700	30	99.6	1016–1042	8.1	6.3
	1625	90	99.6	896–942	12.5	6.1
A4Y13–ASN34	1700	60	99.8	879–1059	8.1	6.5
	1675	60	100	980–1166	7.2	5.8
A4Y13–E10	1725	90	99.5	870–954	13.3	6.4
5% β-Si_3N_4 seed	1700	30	99.3	870–1042	7.2	7.0
	1675	90	99.7	894–1121		
	1625	90	99.3	894–1017	12.7	6.5

*See Table VI footnote for definition of symbols.

given, it represents a statistical average for that property. Where a range of properties is given, there was not enough data generated for a statistical treatment. In general, four to six four-point flexural strength and two or three fracture toughness measurements were made for each composition represented.

The results from Table VII demonstrate that strengths >1 GPa and fracture toughness values of 8–13 MPa·m$^{1/2}$ are possible for several of the Si_3N_4 compositions sintered in the belt furnace. These properties are equivalent to or better than reported for the same or similar compositions which have been sintered at higher temperatures, longer times, and above abient N_2 pressure. These properties are well within the limits required for many automotive applications. What may appear surprising are the high values of flexural strength (>900 MPa) obtained for some compositions where the densities were less than 97% of theoretical. The microstructures for these lower-density materials contain uniformly distributed, well-rounded porosity (generally 3–6 μm in diameter). Because of their small size, the pores do not act as fracture origins and, therefore, are not strength limiting.

Potential for Automotive Applications

An economic comparison has been made between continuous sintering in belt furnaces and conventional sintering in batch furnaces. For two sizes of Si_3N_4 cam-roller followers, belt sintering has been shown to be much more cost effective than batch sintering. Also, the direct and indirect losses are much lower for belt furnaces than for batch furnaces. In general, at high production volumes, sintering in furnaces with graphite hot zones is more cost effective than sintering in furnaces with tungsten hot zones.

For this comparison to be valid, the Si_3N_4 composition must be sinterable under conditions attainable in the belt furnace and have adequate properties for the intended application. The physical property results presented, for a wide range of Si_3N_4 compositions, show that high-strength, tough Si_3N_4 with potential for use in automotive applications can be produced by continuous sintering in a belt furnace.

Acknowledgments

This research was sponsored by the U.S. Department of Energy, Assistant Secretary for Conservation and Renewable Energy, Office of Transportation Systems, as part of the Ceramic Technology for Advanced Heat Engines Project of the Advanced Materials Development Program, under Contract No. DE-AC05-840R21400 with Martin Marietta Energy Systems, Inc. Special thanks to Ceralox, Corp., Molycorp, Inc., and Performance Ceramics for gratis materials used in this research.

References

[1]S. Das and R. Curlee, "The Cost of Silicon Nitride Powder and the Economic Viability of Advanced Ceramics," *Am. Ceram. Soc. Bull.*, **71** [7] 1103–11 (1992).

[2]D. E. Wittmer and C. W. Miller, Jr., "Comparison of Continuous Sintering to Batch Sintering of Si_3N_4," *Am. Ceram. Soc. Bull.*, **70** [9] 1519–27 (1991).

[3]D. E. Wittmer, T. E. Paulson, and C. W. Miller, Jr., "Continuous Sintering of Si_3N_4 in a Controlled Atmosphere Belt Furnace," *Ceram. Eng. Sci. Proc.*, **13** [7–8] 546–62 (1992).

[4]Y. Kalish, "Engine Testing of Ceramic Cam-Roller Followers," Final Report, ORNL/Sub/90-SF985/1, Apr. 1992, 92 pp.

[5]D. E. Wittmer, "Alternative Processing through Turbomilling," *Am. Ceram. Soc. Bull.*, **67** [10] 1670–72 (1988).

[6]D. E. Wittmer and W. Trimble, "Ceramic Composites Processed by Turbomilling"; pp. 273–89 in *Proceedings of the Third International Symposium on Ceramic Materials and Components for Heat Engines* (Las Vegas, NV, Nov. 27–30, 1988). Edited by V. J. Tennary. American Ceramic Society, Westerville, OH, 1989.

[7]D. E. Wittmer and T. E. Paulson, "Evaluation of SiC*w*–Si_3N_4 Composites Containing Beneficiated/Heat-Treated SiC*w*," *Ceram. Eng. Sci. Proc.*, **12** [9–10] 1318–26 (1991).

[8]D. E. Wittmer, D. Doshi, and T. E. Paulson, "Development of β-Si_3N_4 for Self-Reinforced Composites," *Ceram. Eng. Sci. Proc.*, **13** [9–10] 907–17 (1992).

[9]G. M. Crosbie, J. M. Nicholson, and E. D. Stiles, "Sintering Factors for a Dry-Milled Silicon Nitride–Yttria–Alumina Composition," *Am. Ceram. Soc. Bull.*, **68** [6] 1202–206 (1989).

[10]R. F. Cook and B. R. Lawn, "A Modified Indentation Toughness Technique," *J. Am. Ceram. Soc.*, **66** [11] C-200–C-203 (1983).

[11]P. Chantikul, G. R. Anstis, B. R. Lawn, and D. B. Marshall, "A Critical Evaluation of Indentation Techniques for Measuring Fracture Toughness: II, Strength Method," *J. Am. Ceram. Soc.*, **64** [9] 539–43 (1981). ■